SONNE cruise SO 152 : TRACERZIRKEL

28.11.-27.12. 2000

Recife (Brazil) – Pointe a Pitre (Guadeloupe, France)

Chief scientist: Prof. Dr. Monika Rhein
Institut für Umweltphysik, Abt. Ozeanographie   Tel: 49 421 218-2408 (4221)
Otto-Hahn-Allee, Geb. NW1   Fax: 49 421 218-7018
D-28359 Bremen, Germany   email: mrhein@physik.uni-bremen.de

1. Objectives

The objectives of the hydrographic-, tracer- and current meter measurements during SONNE cruise S-152 are:

- Spreading of the deep water masses in the western boundary current
- Estimate of time scales of spreading from recent ventilated deep water from the Labrador Sea into the tropical Atlantic
- Recirculation of the deep water masses in the western tropical Atlantic
- Interhemispheric exchange of water masses
- Continuation of the tracer measurements along 35°W

2. Cruise Narrative

The RV SONNE left Recife on Nov, 28, 8:30 am . While heading north, a test station was carried out in the afternoon. The test of the CTD-O (Conductivity, Temperature, Depth, Oxygen) sonde and the LADCP (Lowered Acoustic Doppler Current Profiler), both attached to a 24-10L bottle Rosette was successful. From the 10L bottles, several water samples are drawn to analyse oxygen, nutrients, salinity, chlorofluorocarbons (CFCs, components CFC-11 and CFC-12), methane (CH_4) , Helium and Tritium. All tracers except helium and tritium were directly analysed on board.

On Nov., 29, 6:00 am the station work began at 7°S, 35°W. At this location, the vessel mounted ADCP was switched on. The vm-ADCP is a new type from RDI, the so called ‚Ocean Surveyor‘, which measures the velocity distribution in the upper 600-650m.

Methyliode is measured continuously from surface water drawn by a special pump system from the ship's well and from atmospheric samples.

The distance between the CTD stations along 35°W was about 20 miles south of 3°N and 30 miles from 3°N to 9°N. We finished the 35°W section at 9°N, 35°W on Dez.7.
On the way to 4°N, 32°34‘W, all 10L bottles were closed in 1000m depth, a region with very low CFC oncentrations to check the bottles for contamination and to check the sampling procedures for the various tracers as well as precision and accuracy of the analysis. The test was successfull.

After Sta. 44 at 4°N, 32°34‘W, the course of the RV Sonne followed mainly the rift valley of the Mid Atlantic Ridge (MAR) to detect hydrothermal activity by anomalies in the methane distributions and in the isotopic signature of the helium samples. At Sta. 46 (6°36‘N, 33°48‘W) the SONNE headed east along a fracture zone and from 9°N, 40°30‘W on the ship followed again the rift valley mainly northward. The station spacing in the rift valley was about 30 miles. On Dec. 13 we encountered the Vema Fracture Zone (VFZ) at 11°N, one of the main passages for deep and bottom water into the eastern Atlantic (Stas. 59-62) . Since the LADCP could only be operated down to 5000m, the transfer through the VFZ occured at locations shallower than 5000m at 10°45‘N, 41°04‘W. First the VFZ was surveyed with Hydrosweep to confirm the topography. 4 CTD-LADCP stations (Stas 59-62) were carried out in the VFZ. Afterwards the SONNE headed further west till Sta. 65 (11°.06N, 43°45‘W

)and then headed north again, following the rift valley till Sta 71 at 14°39'N, 45°00'W. Then the RV SONNE headed west towards Guadeloupe and the ‚16°N' section began at Dec 15 (Stas. 72-124). The horizontal spacing was 30 miles east of 52°W, i.e. above the Midatlantic Ridge. When entering the abyssal plain, the water depth dropped rapidly below 5000m. Therefore, the CTD-Rosette system was alternately lowered down to the bottom without the LADCP and to 5000m with the LADCP attached. The station spacing was 15 miles for the CTD profiles and 30miles for the LADCP and mostly 30 miles for the tracer sampling. After finishing the section with Sta 116 at 60°39'W at Dec 24, station work stopped to celebrate Christmas. At Dec. 25, the boundary current section was repeated with 6 CTD-LADCP profiles but without tracer sampling. The last station, Sta 124 was finished at Dec. 26, 11 am, and the Sonne
arrived in Pointe a Pitre at Dec.26, 4pm.

Next page:
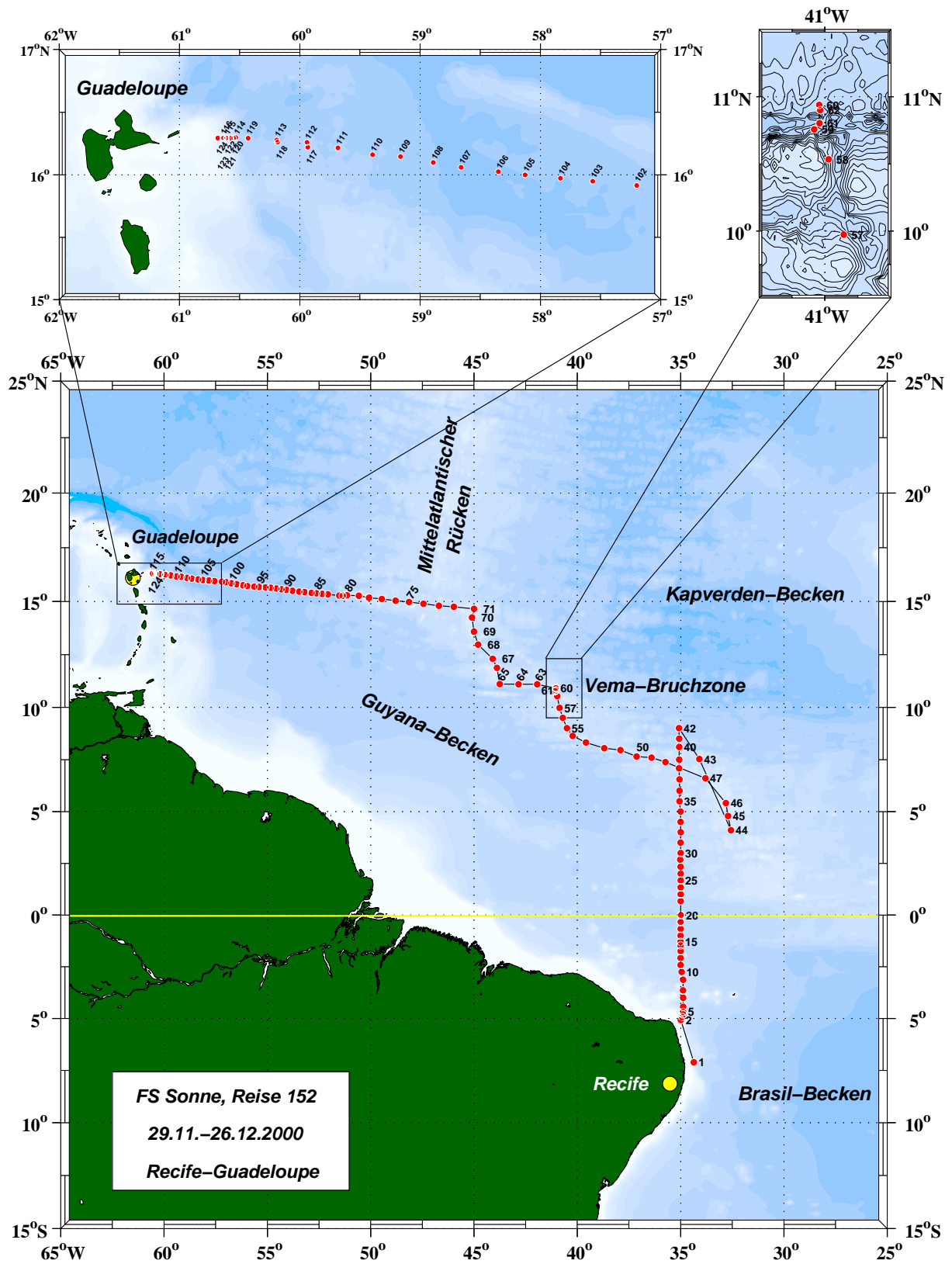Figure 1 cruise track of SONNE cruise S-152 Recife – Pointe a Pitre

Fig.1 Cruise map of RV SONNE , leg SO 152.

3. Results

3.1 The cold limb of the meridional overturning circulation MOC

In the Atlantic, the cold limb of the Meridional Overturning Circulation (MOC) consists mainly of North Atlantic Deep Water (NADW). One of the major components is water formed in the Labrador Sea by convection, the Labrador Sea Water (LSW). Lighter modes are called upper LSW (uLSW), and uLSW might be formed each winter, albeit with different intensities and on different locations (Pickart et al., 1992; Stramma et al., 2003). The denser modes (LSW) are only formed sporadically depending on the climatic conditions and the stratification in the source region (Lazier et al., 2002) . ULSW and LSW form the upper limb of the NADW (upper NADW). The middle and lower NADW consists mainly of overflow water, spilling over the sills between Iceland and Scotland (Iceland Scotland Overflow Water, ISOW) and over the Denmark Strait (Denmark Strait Overflow Water, DSOW). The DSOW part is called lower NADW.

The NADW water masses mainly spread south with the Deep Western Boundary Current. In all DWBC sections made since the early 1980s, a CFC maximum was observed in the upper NADW at about 1600-1800m depth, characterizing uLSW (e.g. Weiss et al., 1985; Rhein et al., 1995; Andrie et al., 2002). The CFCs have been introduced into this water mass by convection. The temporal atmospheric CFC increase is reflected in the temporal CFC increase in this water mass in the DWBC, although modified by mixing and recirculation. This transient CFC signal have been used frequently to estimate transit times (and mean spreading velocities) of the DWBC from the source region to the subtropical and tropical Atlantic (Andrie et al., 2002; Fine et al., 2002).

Since convection activities in the 1970s and 1980s were mainly restricted to the uLSW range, the LSW exhibits no special CFC signal in the tropical Atlantic, but the arrival of CFC enriched LSW, which has been formed between 1988 and 1994 is expected at the equator in the next years (Stramma and Rhein, 2001). A second CFC core around 3800m depth in the lower NADW observed in the DWBC is a feature of the DSOW (Rhein, 1994).

When reaching the equator, both, the upper and the lower CFC core bifurcate, with some of the NADW spreading eastward, and the other part continues with the DWBC along the continental slope of Brazil. The spreading towards the east occur with deep jets, which have been observed with SOFAR floats, deployed in about 1800m depth (Richardson and Fratantoni, 1999).

Since 1990, the hydrographic and CFC distributions along 35°W and along 5°S have been measured as part of international (WOCE repeat hydrography) and national german and french programs. Both sections, along 35°W and along 5°S have been occupied during the same cruise 8 times, with three occupations in October/ November (1990, 1992, 2000) and 5 times in March-June (1991, 1993, 1994, 2000, 2002). Here we present evidence that the spreading of the DWBC waters between these locations shows a seasonal and longer term fluctuations in the upper NADW range (1000 – 2500m depth). No such signal was observed for the deeper limb of the DWBC.

3.2 Variability in the upper NADW, 35°W and 5°S

Details about the 1990-1994 data as well as the measurement techniques and intercomparisons are given in Rhein et al. (1995;1998), and Andrie et al. (1998, 2002).
Both sections, the 35°W and the 5°S section have been sampled during METEOR cruises M14 (October 1990), M16 (June 1991), M22 (November 1992), M27 (March 1994), M47 (March 2000), M53 (June 2002) , the CITHER 1 cruise (March 1993). The data from October – November 2000 were taken during two subsequent cruises with the german research vessel SONNE (cruises S151 and S152), the data from June 2002 were taken during cruise M53/2 with RV METEOR.

Mean CFC profiles for the NADW were calculated by interpolating the data on a regular vertical and horizontal grid before averaging them horizontally. The grid spacing depended on the spatial data resolution and was largest on the M16 cruise (June 1991), and lowest for the more recent data. At 35°W, the region from the continental slope to the equator was averaged, and at 5°S the area from the continental slope to 33.5°W was taken. Different choices of the horizontal extension (to 3°N at 35°W, to 32°W at 5°S) do not change the general features presented. The mean standard deviation of the presented profiles is about 0.01 pmol/kg.
If one compares only the CFC concentrations from the 35°W cores with the 5°S cores, the concentration differences are significant in March 1993, 1994, 2000 and in June 2002, and almost equal in October 1990, November 1992, and 2000. In June 1991, the spatial resolution both, horizontal and vertical, was too sparse to resolve features (Andrie et al., 2002).

3.2.1 The upper NADW
In the tropical Atlantic, the CFC maximum of the uLSW is centered at 1600-1800m depth (Figures 2, 3). At 35°W, due to the interaction of the DWBC with the local equatorial dynamics, the CFC core is split in several maxima , and these features are observed in all occupations of the 35°W sections (Rhein et al., 1998; Andrie et al., 2002). The CFC cores roughly coincides with the velocity distribution. The latter was studied by Schott et al. (2003) using 9 shipboard current profiling sections. The found the strongest eastward flowing current branch located offshore at 1.5°S-3.5°S , and another one between 1°N and 3°N and these locations are marked with high CFC values (Figure 2).

Part of the CFC bearing water masses continues with the DWBC at the continental slope towards the south . The direct path for the uLSW between the 35°W and the 5°S section is only about 120 nautical miles. Even with a lower limit velocity of 1-2 cm/s (Richardson and Fratantoni, 1999) the time needed for transit is shorter than 1 year. One would expect a negligible transient CFC signal and the CFC concentrations should be similar on those two locations, provided that mixing with CFC poor water can be neglected. In November 2000, the CFC concentrations in the uLSW are similar at 35°W and at 5°S (Figures 2a, 3a). In June 2002, however, the CFC concentrations along 5°S are significantly smaller than the ones at 35°W (Figures 2b, 3b).

3.2.2The lower NADW
The CFC maximum at 3700-4000m depth characterises the Denmark Strait Overflow Water (DSOW). At 35°W, the deep CFC core coincides with the velocity core (Rhein et al., 1995; Schott et al., 2003). The flow is restricted by topography to pass the 35°W section at the northern flank of the Equatorial channel north of 1°40'S. Both, the velocity and the CFC signal of the DSOW, are lower at 5°S compared to 35°W, and the T/S characteristic also change significantly (Rhein et al., 1995). This indicates either strong mixing or the core at the Equatorial channel does not continue directly to 5°S. East of 35°W, the direct flow to the
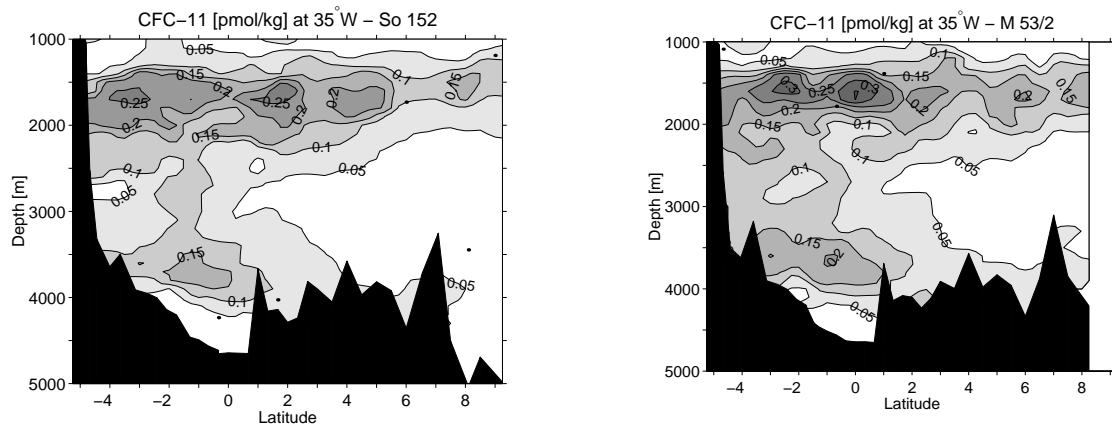
Figure 2 CFC distribution along 35°W from Brazil to the Mid-Atlantic Ridge, a) November 2000, cruise S152; b) June 2002, cruise M53/2
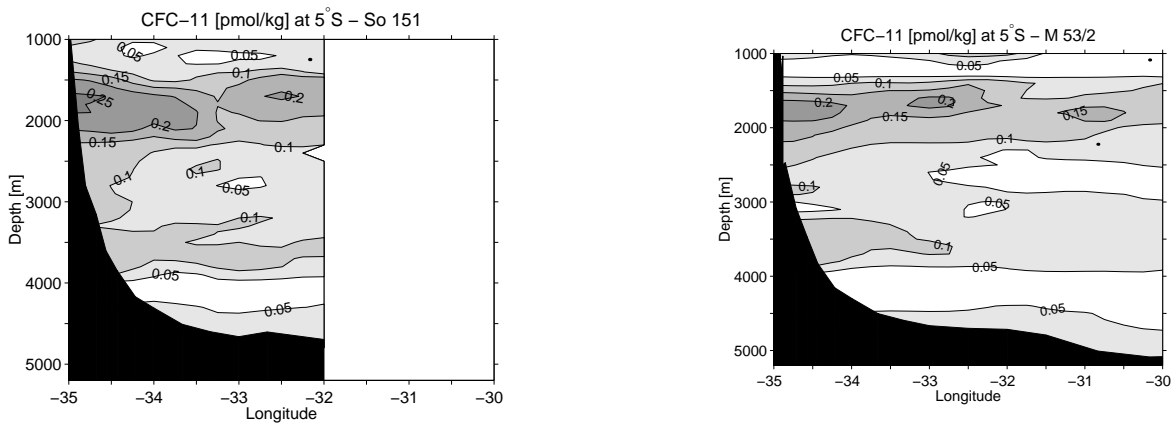

Figure 3 CFC distribution along 5°S from Brazil to 30°W. a) November 2000, cruise S151; b) June 2002, cruise M53/2

south is restricted by a chain of submarine mountains around the Atoll das Rocas at 3°S – 4°S. The elevated topography extends from 34°W to 31.5°W , leaving only a gap of about 30 miles between the continental slope and east of 34.5°W which is deeper than 3500m (Figure 1). The highest CFC concentrations at 5°S, are always found near the continental slope (Figure 2), indicating that this small gap transports some of the deep CFC signal south, which is then mixed and diluted with CFC poorer water. The deep CFC tongue extends from the continental slope as far east as 32°W.

3.2.3 Seasonal signal in the CFC distributions

One surprising feature in the CFC distribution in the uLSW layer was already noted by Rhein et al. (1998). In spring 1994, they found a significant CFC decrease from 35°W to 5°S, supported by independent oxygen and tritium measurements. In the observations 1990-1992, the CFC values of the 35°W and the 5°S sections were similar, and Rhein et al. 1998 treated the 1994 observations as an exception.

In view of the 8 CFC sections along 35°W and 5°S (Figure 4), the 1994 result is seen in a different light. In the uLSW layer between 1100 and 2500m depth, the mean CFC concentrations decrease downstream from 35°W to 5°S during spring/summer in 1993, 1994, 2000, and 2002. The CFC values at 35°W and 5°S were equal within the uncertainty of the data in the autumn sections : October 1990, November 1992, and November 2000. The exception seems to be June 1991, but as mentioned above, the spatial and vertical resolution of the CFC data during that cruise were much lower than during the other cruises, probably obscuring the signal.

For the lower CFC core of the DSOW, the CFC concentrations at 5°S are substantially lower (except in March 2000 and November 2000, where they were about equal) than at 35°W, and no seasonal signal can be depicted (Figure 4).

SOFAR floats from Richardson and Fratantoni (1999) revealed three equatorial jets: two eastward flowing jets located between 1°N - 3°N (northern jet) and 1°S – 3°S (southern jet), respectively, interspersed by a westward jet between 1°S and 1°N. At the 35°W sections, the location of the southern jet coincides with the the major uNADW current branch found by Schott et al (2003) and with a CFC core. Float trajectories confirmed, that part of the water in the southern jet at 35°W continues eastward, carrying the CFC signal towards the east, and part continues southward (Richardson and Fratantoni, 1999). Although the evidence of a seasonal variation in the monthly mean velocities east of 40°W of the southern jet is poor, higher than average eastward velocities were found in February – June, and lower than average velocities in August – November. The float data confirmed the conclusions derived from shipboard current profiling along 35 °W and from moored instruments at 44°W: low eastward transports in the upper NADW during September/October, high eastward transports in January/February (Fischer and Schott, 1997).

Lower eastward velocities might allow enough CFC enriched water to flow south in autumn and to keep the CFC concentrations at 35°W and 5°S at the same level, despite the autumn transport minimum west of 35°W. The higher eastward velocities in spring/summer east of 35°W presumably transport the major part of the CFC core eastward along the equator, causing less CFC rich water to flow in the DWBC at 5°S, despite the transport maximum west of 35°W.
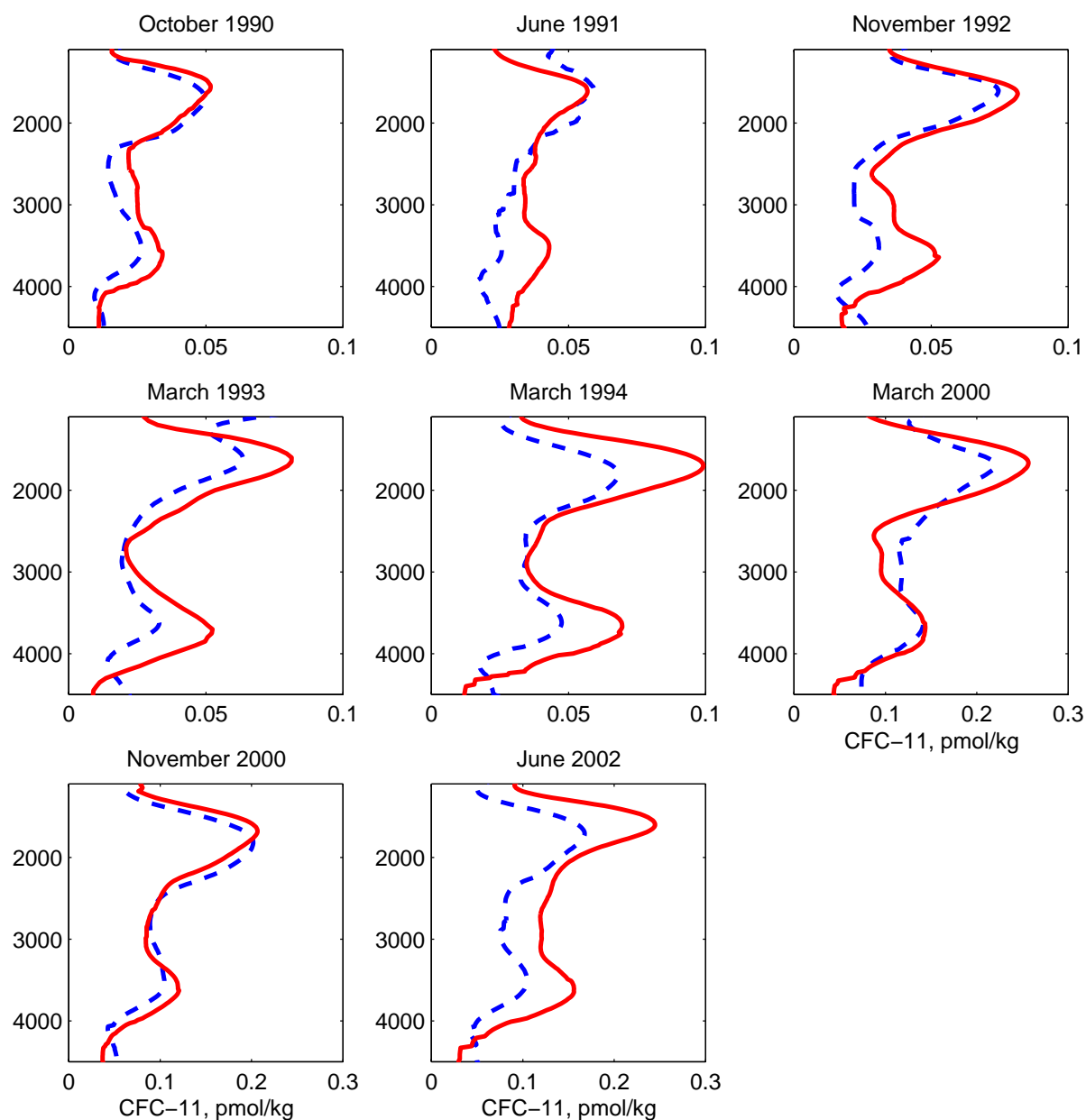
Figure 4 Mean CFC profiles at 35°W (bold) and at 5°S (stippled). Details about the averaging methods see text. Note the changing scale of the x axis starting in November 2000

3.2.4. Indications for longer term fluctuations in the upper NADW

A comparison of the mean CFC concentrations in the core of the upper NADW at the 2000-2002 data reveal indications for longer than seasonal fluctuations.

The year 2000 is the only one with a data set in spring and in autumn. At 35°W, the mean CFC concentrations in the core of the upper NADW was 0.26pmol/kg in March, compared to 0.2 pmol/kg in November. At 5°S, the CFC values were 0.22pmol/kg in March, and 0.2pmol/kg in November. In June 2002, the CFC concentrations at 35°W were almost as high as in March 2000 (0.25pmol/kg). At 5°S, however, the CFC concentrations decreased fin the time period 2000-2002 from 0.2pmol/kg to 0.17pmol/kg .

It seems that the high CFC signal observed at 35°W in March 2000 did not reach the 5°S section. The CFC decrease at 5°S from the year 2000 to 2002 might even indicate that during that time period most of the CFC enriched water did not flow south with the DWBC.

10

The SOFAR float trajectories (Richardson and Fratantoni, 1999) suggested, that at times the DWBC flows directly southward across the equator. At other times, the DWBC water is diverted eastward near the equator for longer periods (1-2 years), which can reduce the mean along boundary velocity from 8-9cm/s to 1-2cm/s.

3.4 Zonal currents and transports at 35°W

3.4.1 The deep circulation

The zonal velocity distribution along the 35°W section is presented in Figure 5. At 35°W, the current field is complicated due to the encounter of the DWBC with the mainly zonal equatorial circulation (see 3.2). The upper NADW and LSW layers are split in several eastward flowing velocity cores, separated by westward flowing branches. Usually one finds directly along the boundary the continuation of the eastward flowing DWBC (Schott et al., 2003), but this branch was absent in November 2000. A second branch is located offshore at 1.5°-3.5°S (Fig.4), and this flow path seems to be a permanent feature of the deep flow. The flow of the lower NADW and AABW is forced by topography to flow along the equatorial channel between 1°40'S and 0°40'N, and the main veloctiy core is located on the southern side of the channel. The AABW passes westward underneath the lower NADW. Schott et al. (2003) used 13 shipboard current sections along 35°W to determine the mean meridional structure of the zonal circulation and to calculate mean transports. For the NADW layers, the net transport is 22 Sv to the east. The upper NADW and LSW level (1200-2500m depth), however, contributes only a small fraction of the net flow (2.9 Sv), with 17.8 Sv flowing eastward and 14.9 Sv flowing westward. This suggests, that the main contribution to the deep northern hemispheric meridional overturning circulation come from the middle and the lower NADW (2500-4000m). The westward AABW transport amounts to 2 Sv, somewhat higher than the 1.5-1.8 Sv of Rhein et al. (1998).
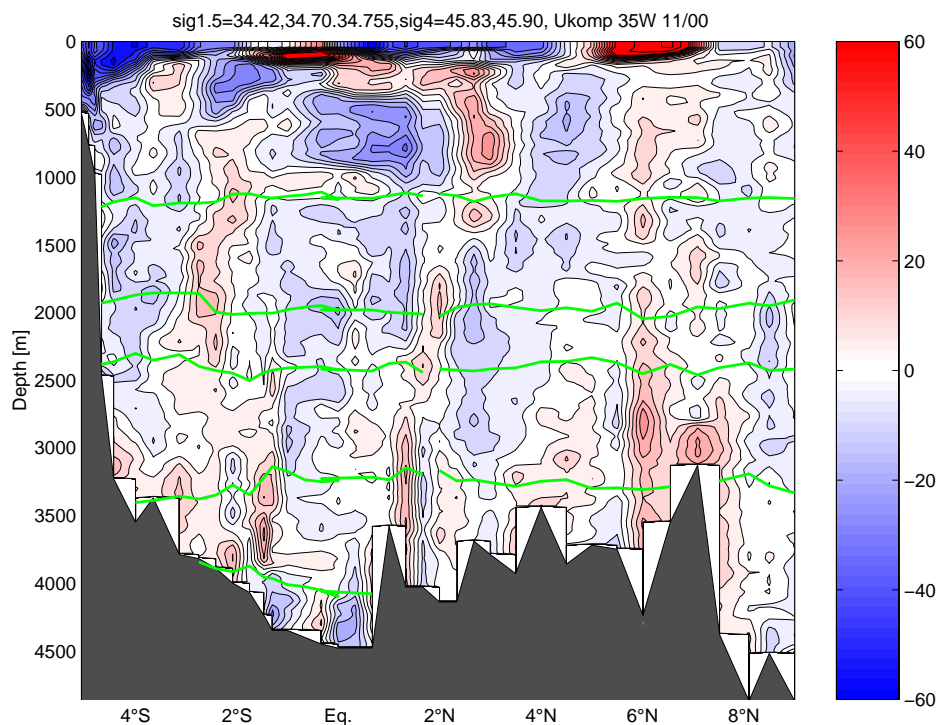

sig1.5=34.42,34.70.34.755,sig4=45.83,45.90, Ukomp 35W 11/00

Figure 5 *zonal velocity component along the 35°W section, SONNE cruise S-152. Left side: Brazil, right side: Mid Atlantic ridge. Red: eastward velocity, blue: westward velocity, velocity in cm/s. The green lines are isopycnals (chosen from Rhein et al., 1995) to separate the deep water masses upper NADW (1200-1900m), LSW(1900-2500m), middle NADW(2500-3400m), lower NADW(3400-4000m) and Antarctic Bottom Water AABW (below 4000m).*

3.4.2 The upper circulation

The upper circulation along 35°W in November 2000 was measured with the 75kHz vessel mounted Ocean Surveyor (Fig.6). The North Brazil Current (NBC) is located at the brasilian coast and transports about 22Sv westward and no clear separation exists between the SEC South Equatorial Current) and the NBC. The SEC extends to 3°N and transports another 14.7 Sv towards the west. The EUC (Equatorial Undercurrent) hast ist maximum velocity in 100-150m depth (higher than 1m/s) and transports 13.1 Sv eastward, close to the mean of 12.3 Sv found by Schott et al. (2003). The SEUC (South Equatorial Undercurrent) located between 3°-4°S flows eastward with 5.3 Sv -- almost double the mean transport of 2.8 Sv) and the transport of the NEUC (North Equatorial Undercurrent) amounts to 8.7 Sv.
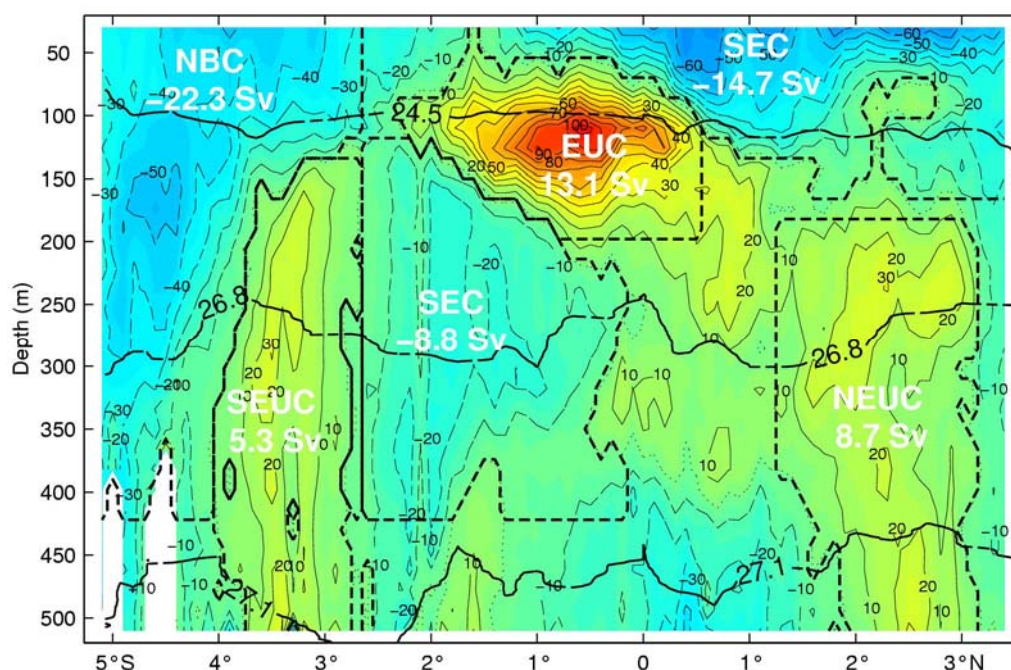

Figure 6 Zonal velocity component from the vessel mounted 75kHz Ocean Surveyor. The bold dark lies are isopynals, separating the Subtropical salinity maximum water from the central water masses. Below the sigth= 27.1, the Antarctic Intermediate Water (AAIW) is located. Positive: eastward flow, negative: westward flow.

3.5 Spreading of deep water masses derived from CFC age distributions

The 'young' components of the NADW, the Upper (UNADW) and Lower (LNADW) North Atlantic Deep Water, are marked by a maximum of the concentration of the chlorofluorocarbons CFC-11 and CFC-12 (Andrié et al., 2002). The CFCs are transient tracers, the increase of their atmospheric mixing ratio is reflected by the CFC-concentration in the NADW. This increase contains a time information about the export of NADW from its source region into the tropics, which can be extracted by analysing the measured data.
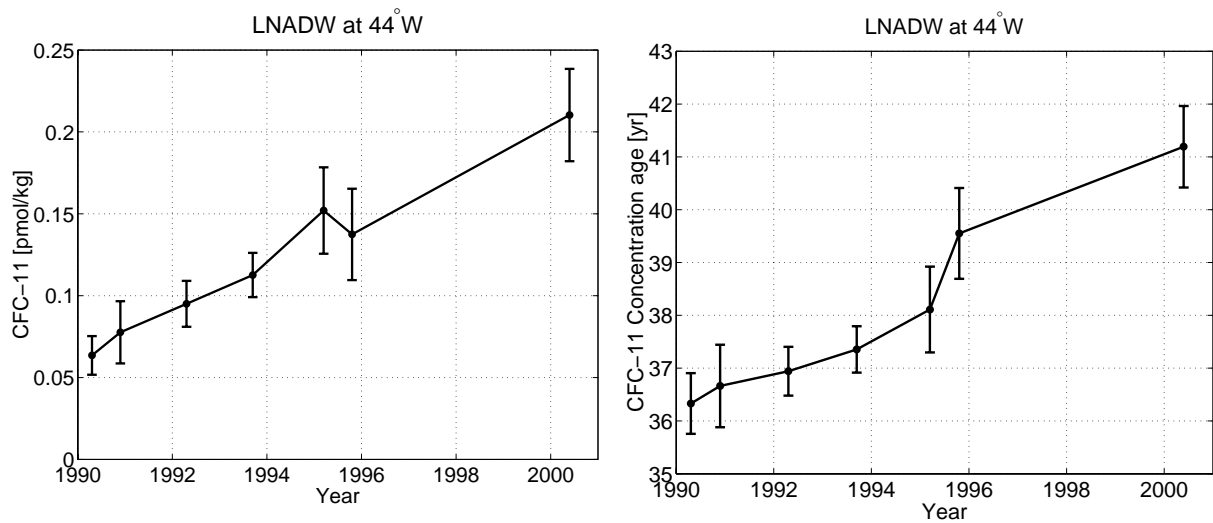

Fig.7: CFC-11 concentration (left) and CFC-11 concentration age (right) in the LNADW density range for the repeated sections at 44°W in the tropical Atlantic.

Concentration Age

The concept of 'ages' can be used to interpret the transient CFC-signal in the ocean interior. The age of a water mass is the time elapsed since its formation, i.e. when the water was last exposed to the atmosphere. The time of water mass formation according to the concept of concentration age is determined as the year when the measured oceanic CFC-concentration equals the solubility equilibrium of the atmospheric CFC-mixing ratio (Doney and Bullister, 1992). Normally, however, the newly formed water is undersaturated with respect to CFCs because of the entrainment of older water during the formation process. In the Labrador Sea, for example, the concentration age of Labrador Sea Water (LSW) is about 10 years. This can be taken into consideration by substracting the 'relic' age from the calculated concentration age.

In the tropical Atlantic, mean core concentrations of CFCs are calculated for the density ranges of UNADW, LSW and LNADW at the specific sections. Fig.7 shows the results for the repeated measurements at 44°W within the LNADW layer. The CFC-11 concentration shows an increase from 0.05 to 0.2 pmol/kg over the observational period from 1990 to 2001. The CFC-concentration age is not exactly constant in time. The change from 36 to 41 years, however, is comparatively low. This change may be due to variability of NADW transport, but it is also a consequence of the nonlinear behaviour of the concentration age under mixing processes in the ocean interior.

Age Spectra in the Tropical Atlantic

The concept of age spectra (Hall and Plumb, 1994) considers both the change of the atmospheric CFC-content and the transport and mixing processes in the ocean. Therefore a water parcel is considered as a composition of infinitesimal fluid elements with different ages and CFC-concentrations. The age spectra describe the distribution density of ages within the water parcel. For a 1-dimensional, steady state circulation an analytical solution for the age spectra exists. This analytical expression fulfills the advection-diffusion equation and depends on the velocity u and diffusivity k of the flow. Additionally, the mixing of NADW with 'old' water free of CFCs (e.g. water of Antarctic origin) is accounted for by a dilution factor f ($0 < f$ 1). The parameters u, k, and f are fitted by minimizing the deviation between the CFC-concentrations computed by the age spectra and the measured values. In accordance to the 1-dimensional solution, u and k are the same for each water mass at all sections. The fraction f is varying from section to section, but only solution with downstream decreasing values of f are acceptable.

A range of values has been determined for the parameters u, k and f, yielding the observed evolution of CFC-concentrations. It is not possible to give a reliable estimation of the diffusivity k, possible values range from 100 to 10000 m²/s. The velocity, however, is restricted to a relatively small interval from 1.5 to 2.0 m/s. These values are comparable to earlier results based on the interpretation of CFC-data in the tropical Atlantic (Andrié et al., 2002). The fraction f of pure NADW shows the required southward decrease, indicating the mixing of NADW with water from Antarctica (Fig.8).

The signal of enhanced LSW formation, resulting from intense deep convection from 1972 to 1976 and 1988 to 1994 in the Labrador Sea, should be reflected by a strong increase of CFCs in the LSW-range in the tropical Atlantic (Freudenthal and Andrié, 2002). Near the equator, however, this signal is overlaid by the variability of the equatorial current system. Transient Equatorial Deep Jets export NADW into the eastern Atlantic, leading to a sporadic decrease of CFC-content in the Deep Western Boundary Current.

For the northernmost section at 16°N, where the signal of LSW is expected to be strongest, only two realisations have been carried out so far in 2000 and 2002. Assuming a mean current speed of about 1.5 cm/s, the LSW-signal from the 1970s has already passed the 16°N section, whereas the signal from the late 1980s will arrive not before 2005. Repeated measurements at this section therefore provide a good means to test the estimation of spreading velocities for NADW.
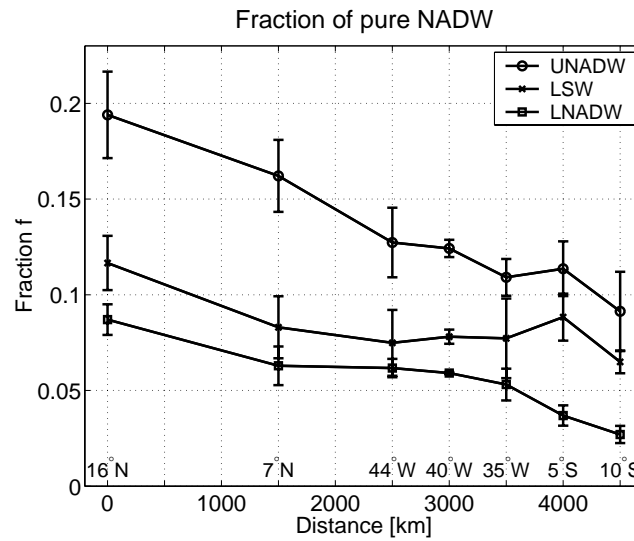
Fig.8: Fraction f of pure NADW for UNADW, LSW and LNADW. The belonging values for velocity and diffusivity are k = 1000 m²/s and u = 1.5 cm/s for UNADW and LSW and 2.0 cm/s for LNADW.

3.6 Helium and Methane anomalies, SONNE cruise S-152

In close cooperation with R. Keir (GEOMAR) the Helium and methane anomalies in two different regions at the MAR were studied in December 2000 (Mid Atlantic Ridge between 4°N and 16°N, RV Sonne cruise S-152). The $^3He/^4He$ ratio of midocean hydrothermal fluids are 8-30 times enriched relative to atmospheric helium: the atmospheric ratio Ra is $1.4x10^{-6}$, the ratio of submarine hydrothermal fluids injected from deep sea spreading ridges and from several active seamounts is about 7-20 Ra. The basalts of spreading ridge systems have $^3He/^4He$ ratios of 9.14+-3.59 Ra, the highest ratios are found along ridge systems associated with new ridges, and low values are associated with long lived or abandoned ridges (Anderson, 2000). Hot spot areas such as Iceland or Hawaii show $^3He/^4He$ ratios up to 20-30 Ra, for instance, the Helium isotopes emanating from the Loihi Seamount near Hawaii have ratios between 23-27 Ra (Lupton, 1998).

Typical hydrothermal fluids have ^3He concentrations ranging from 0.2 to $2.5x10^{-9}$ cm³ STP/g (STP Standard Temperature and Pressure), several orders of magnitude higher than the oceanic background (about $6x10^{-14}$ cm³ STP/g), (Lupton, 1998; Butterfield et al., 1990). Because ^3He has such a high concentration in the hydrothermal vent fluids, ^3He can be used to trace hydrothermal plumes for thousands of kilometers from the source regions.

Early measurements within the GEOSECS program showed little evidence of primordial ^3He input at the MAR (eg Jenkins and Clarke, 1976). Broecker (1980), however reported on a small ^3He excess at one location in the Brazil Basin, which he associated with a ^3He input at the MAR. In the meantime, several hydrothermal vents have been found in the North Atlantic, for instance the Logatchev vent field at 14°45'N (eg Sudarikov and Rouminatsev, 2000), the TAG hydrothermal field at 26°N (Rona et al., 1984) Snakepit at 23°N (Kong et al., 1985), and Lucky Strike at 37°17'N (e.g. Jean-Baptiste et al., 1998).

So far, no hydrothermal vent fields have been identified south of 14°N. There are however strong indications from ³He measurements in the water column that several hydrothermal vents exist in the Southern Atlantic at the Mid-Atlantic ridge (Rüth et al., 2000).

Hydrothermal venting should lead to anomalies in both, the helium and the methane distribution. The serpentinization of ultramafic rocks, however, generate methane anomalies, but no helium signal. As an example for the tropical part of the MAR, the methane and helium values from three locations in the rift valley of the MAR near 4°N are compared with the helium profiles from the Vema Fracture zone and just north of the fracture zone (Fig. 9)
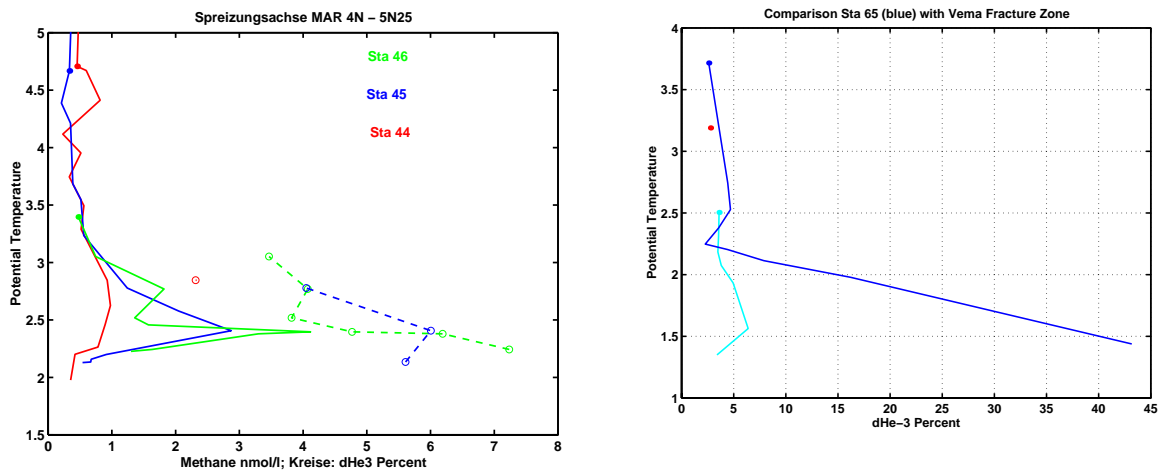

Figure 9 helium and methane profiles from the MAR: left 4°N – 5.5°N, bold lines: methane, stippled lines: helium. Right side: helium in the Vema fracture zone (light blue line), the high values at the bottom of more than 40% are from the spreading axis just north of the Vfz (dark blue line). Note the different scale of the xaxis.

Between 4°N and 5.5°N, a significant methane anomaly at temperatures around 2.5°C are accompanied by a weak helium anomaly, indicating that serpentinization of ultramafic rocks may play a significant role. The high helium anomaly at the bottom of the spreading axis at 11°6'N (Fig. 9b) is correlated to a very weak methane signal (not shown), indicating the presence of an active hydrothermal vent nearby. These results were presented at the AGU fall meeting in 2001, a manuscript (Keir, Rhein, Wallace, Greinert) is in preparation.

All methane – helium correlations measured in the fracture zones ans rift valley of the MAR are presented in Figure 10.
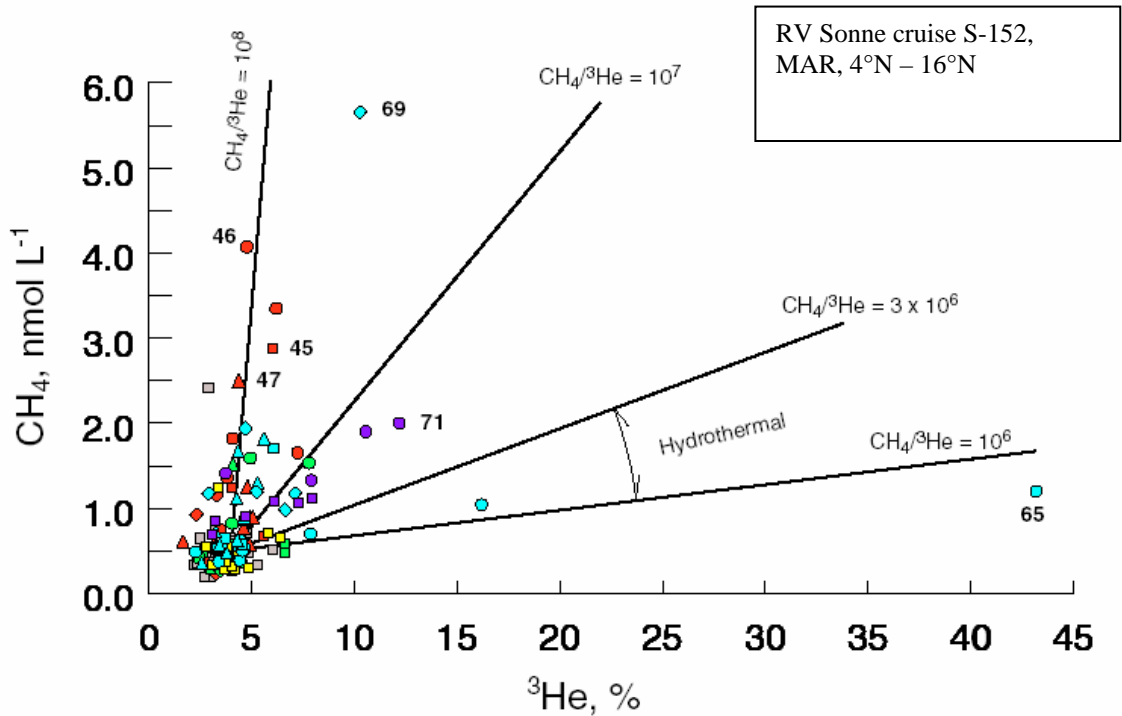

Figure 10 Methane concentrations vs delta-^{3}He anomalies, locations between 4°N and 14°N. The numbers are station numbers. The stations with hydrothermal relations are found in the rift valley at 11°6'N, the stations with the strongest methane concentrations (Stas 45-47) are located in the rift valley between 4°N and 5.25'N. Station 69 is located bei 14°40'N south of Logatchev. The spatial resolution of the measurements was between20 and 50 nautical miles, much too high to resolve the exact location of hydrothermal vents.

3.7 The warm limb of the Meridional Overturning Circulation

The upper part of the thermohaline circulation in the tropical Atlantic consists of warm water from the South Atlantic. It enters the Northern Atlantic mainly in the North Brazil Undercurrent (NBUC) and the South Equatorial Current (SEC). Both currents combine between 35°W and 40°W and create the North Brazil Current (NBC), flowing along the Brazilian coast (Schott et al., 1995; 1998). Part of the NBC joins the zonal equatorial flows. North of the retroflection zone of the NBC-NECC (North Equatorial Counter Current) the northward transport of warm water mainly occurs in eddies (Didden and Schott, 1993), the transport is therefore difficult to assess.

The NBC transport is much higher than the net interhemispheric water exchange. Part of the NBC flows back into the South Atlantic through the equatorial current system. Owing to significant variability in the transport and divergences in the wind field, the net exchange cannot be measured easily. Ultimately, the southern hemispheric water which remains in the North Atlantic, flows into the Caribbean and joins the Florida Current. Part of the water may also flow east of the Caribbean towards the north.

The warm water limb comprises several water masses. The Salinity Maximum Water (SMW) between 50 and 100m depth is embedded in the Tropical Surface Water (TSW) reaching from the surface to the sigma_theta = 25.6 isopycnal. This isopycnal represents the 20°C isotherm, which is frequently used to define the lower limit of the TSW. The SMW is subducted in the subtropical South Atlantic where it gained the high salinity values at the surface. Below the TSW, the South Atlantic Central Water (SACW) is found, its lower limit is the sigma_theta= 27.1 isopycnal. The sigma_theta = 26.8 separates the zone with weak vertical gradients from the denser part with strong vertical gradients. The profiles in the northern part of the section show significant contributions of North Atlantic Central Water (NACW).
The salinity minimum centered at 800m depth characterizes the Antarctic Intermediate Water (AAIW). The AAIW flows westward with the NBC and EIC, and part of it recirculates north of 5°N and flows eastward with the NICC between 5°N and 6°N. The AAIW carries ist salinity minimum into the subtropical North Atlantic and is a significant feature as far north as 40°N.

To determine the fraction of South Atlantic water in the data of the S-152 and S-151 cruise, iospycnal mixing was assumed and the fraction was calculated from the distribution of potential temperature and salinity (Fig.11). The source water masses are SACW (South Atlantic Central Water) and NACW (North Atlantic Central Water). SACW was defined at 10°S off Brazil (cruise S-171), similar to the definition from Poole and Tomczak (1999). The deep part of the NACW was defined at 24°N (WOCE section A05, 1992), for lower densities S-152 measurements at 16°N, 57°W (S-152 cruise) were used. The 24°N data were used because the S-152 salinities were lower than the definition of Poole and Tomzcak. In the density layers of the SMW, the influence of a source water mass from the eastern equatorial Atlantic was noted, and the characteristic of this water (named ESW) was defined from measurements at 2°N, 23°W (cruise M47). The density layers chosen were a) Salinity maximum water SMW (25.5<sigma<26.3); b) upper central water (26.3<sigma<26.8), c) lower central water (26.8<sigma<27.1), and d) intermediate water (27.1<sigma<27.4). Densities shallower than sigma=25.5 could not be included in the calculation, since they outcrop in the research region (Fig.). Thus the SMW layer only includes the densities below the salinity maximum.
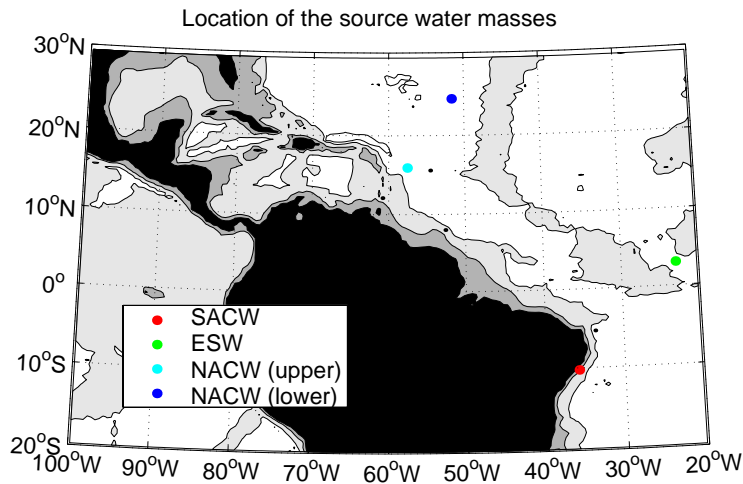
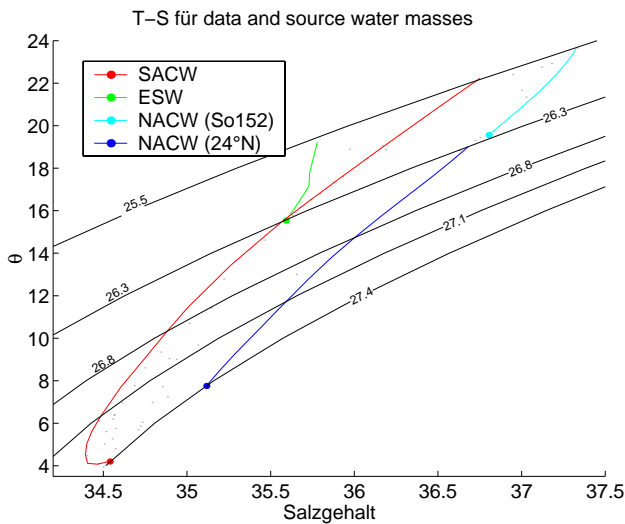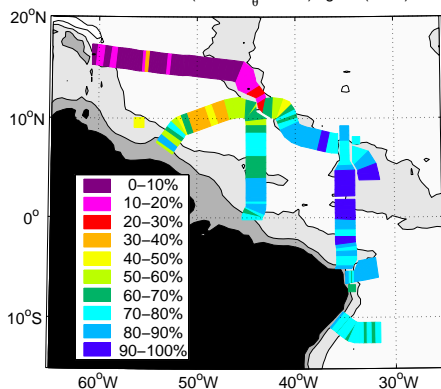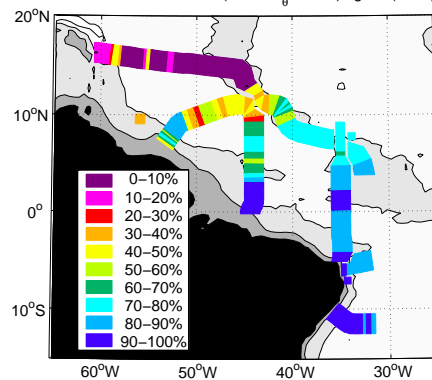*Figure 11 Location of the source water masses*

Figure 12 T-S diagram for the data and source water masses. The uppermost layer encompasses the lower part of the salinity maximum water.
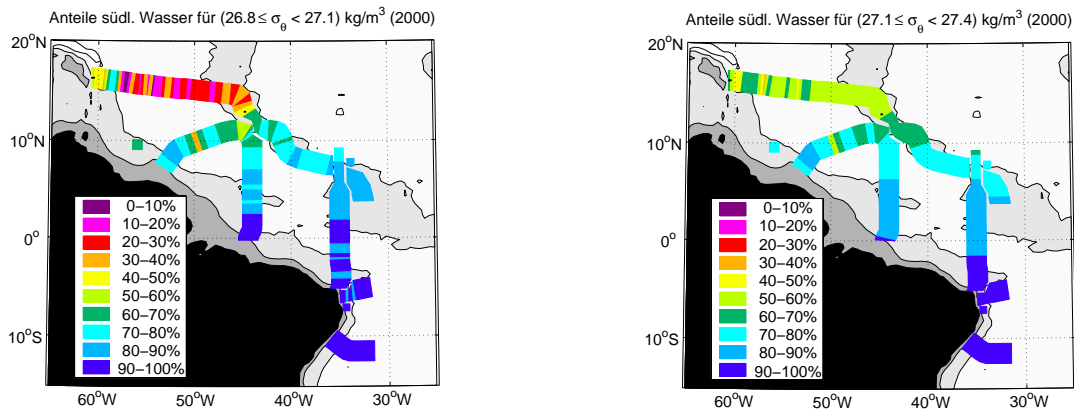
Figure 13 Fraction (in percent) of water from the South Atlantic, S-152 and S-151 data.a) salinity maximum water, b) upper central water, c) lower central water; d) Intermediate water

For the Salinity maximum water (Fig. 13a) the contribution of southern hemispheric water at the 16°N section is lower than 20% . In the upper central water (Fig.13b), up to 50% are found on some location, but in general, the fraction is lower than 20%. For both water masses, the difference between the 7°30N section and the 16°N section is striking, the fraction of South Atlantic water decreases about 50-70% to lower than 20%, indicating a possible transport of the southern hemispheric water into the Caribbean trough the passages between Guadeloupe and South America.

For the lower central water, however, the contribution from the South Atlantic at 16°N are mostly between 20-40% (Fig. 13c), and in the intermediate water range about 50-70% are from the South Atlantic. This is the northward flowing Antarctic Intermediate Water (AAIW), which carries a salinity minimum from ist source region in the circumpolar current into the subtropical North Atlantic. For both water masses, the inflow into the Caribbean is more restricted by the topography, by limited depths of the passages and limited area of the throughflow.

At the 35°W section and further east and south, the southern hemispheric water contributes more than 70-80% .

References

Anderson, D.L., The statistics of Helium isotopes along the global spreading ridge system and the central Limit Theorem. Geophys. Res. Lett. 27, 2401-2404, 2000.

Andrie, C., J.F. Ternon, M.J. Messias, L. Memery, and B. Bourles, Chlorfluoromethanes distributions in the deep equatorial Atlantic during January – March 1993. Deep-Sea Res. I 45, 903-930, 1998.

Andrie, C., M.Rhein, C.Freudenthal und O.Plähn, CFC time series in the deep water masses of the tropical Atlantic, 1990-99. Deep Sea Res I, 49, 281-304, 2002

Doney, S.C und J. Bullister, A chlorofluorocarbon section section in the eastern North Atlantic, Deep Sea Res., 391857-1883, 1992

Fine, R.A., M. Rhein, and C.Andrie, Storage of climate properties in the deep western North Atlantic Ocean. Geophys. Res. Lett., 29, 10.1029/2002GL015618, 2002.

Fine, R., M. Rhein und C.Andrie, Using a CFC effective age to estimate propagation and storage of climate anomalies in the deep western North Atlantic Ocean. Geophys. Res. Lett. 29, No. 24, doi:10.1029/2002GL015618, 2002.

Fischer, J., and F.A. Schott, Seasonal transport variability of the deep western boundary current in the equatorial Atlantic. J. Geophys. Res. 102, 27.751-27.769, 1997

Freudenthal, S. und C. Andrié, The arrival of a 'new' Labrador Sea Water signal in the tropical Atlantic in 1996, Geophys. Res. Lett., 29(0), 10.1029/2002GL015062, 2002

Hall, T.M. und R.A. Plumb, Age as a diagnostic of stratospheric transport, J. Geophys. Res., 99, 1059 -1070, 1994

Jean-Baptiste, P.H. Bougault, A,Vangriesheim, J.L., Charlou, J.Radford-Knoery, Y.Fouquet, D.Needham, and C. German, Mantle ^{3}He in hydrothermal vents and plume of the Lucky Strike site (MAR, 37°17'N) and associated geothermal flux. Earth Planet. Sci. Lett. 157, 69-77, 1998.

Kurz, M.D., W.J. Jenkins, J.G. Schilling, S.R. Hart, Helium isotope variations in the mantle beneath the central North Atlantic Ocean. Earth. Planet. Sci. Lett. 58, 1-14, 1982.

Lupton, J. Hydrothermal helium plumes in the Pacific Ocean. J.Geophys.Res. 103, NoC8, 15.835-15.868, 1998

Lazier, J., R. Hendry, A. Clarke, I. Yashayaev, and P. Rhines, Convection and restratification in the Labrador Sea, 1990-2000. Deep-Sea Res. I, 49, 1819-1835, 2002

Pickart, R.S., Water mass components of the North Atlantic Deep Western Boundary Current. Deep-Sea Res. I 39, 1553-1572, 1992.

Poreda, R.J., J.G. Schilling, H. Craig, Helium and hydrogen isotopes in ocean ridge basalts north and south of Iceland. Earth Planet. Sci. Lett. 78, 1-17, 1986.

Poreda, R.J., H. Craig, S. Arnorson, J.A. Welham, Helium isotopes in Icelandic geothermal systems I: ³He, gas chemistry and C-13 relations. Geochim. Cosmochim. Acta 56, 4221-4228, 1992.

Rhein, M., The deep western boundary current: tracers and velocities. Deep-Sea Res. I 41, 263-281, 1994.

Rhein, M., L. Stramma, and U. Send, The Atlantic deep western boundary current: water masses and transports near the equator. J. Geophys. Res. 100, 2441-2457, 1995

Rhein, M., O. Plähn, R. Bayer, L. Stramma, und M. Arnold, The temporal evolution of the tracer signal in the Deep Western Boundary Current, tropical Atlantic, J. Geophys. Res., 103C,15.869-15.884, 1998

Rudnicki, M.D. and H. Elderfield, Helium, radon and manganese at the TAG and Snakepit hydrothermal vent fields, 26°N and 23°N, Mid Atlantic ridge. Earth Planet. Sci. Lett. 113, 307-321.

Rüth, C., R.Well, and W. Roether, Primordial ³He in South Atlantic deep waters from sources on the Mid Atlantic ridge. Deep Sea Res. I 47, 1059-1075, 2000.

Rona, P.A., G.Thomson, M.J. Mottl, J.A. .Karson, W.J. Jenkins, D.Graham, M.Malette, J.VonDamm, J.M. Edmond, Hydrothermal activity at the TAG hydrothermal field, Mid Atlantic Ridge crest at 26°N. J.Geophys. Res., 89, 11365-11377

Richardson, P.L., and D.M. Fratantoni, Float trajectories in the deep western boundary current and deep equatorial jets of the tropical Atlantic. Deep-Sea Res. II, 46, 305-333, 1999.

Schott, F., M.Dengler, L. P. Brandt, K.Affler, J. Fischer, B. Bourles, Y. Gouriou, R.L. Molinari and M. Rhein, The zonal currents and transports at 35°W in the tropical Atlantic. Geophys. Res. Lett., in press, Jan 2003.

Stramma, L., and M. Rhein, Variability in the Deep Western Boundary Current in the equatorial Atlantic at 44°W. Geophys. Res. Lett., 28, 1623-1626, 2001.

Stramma, L., D. Kieke, M. Rhein, F. Schott, I. Yashayaev, and K.P. Koltermann, Recent deep water changes at the western boundary of the subpolar North Atlantic. To be submitted.

Sudarikov, S.M., and A.B. Roumiantsev, Structure of hydrothermal plumes at the Logatchev vent field, 14°45'N, Mid Atlantic Ridge: evidence from geochemical and geopysical data. J. Volcan. Geotherm. Res. 101, 245-252, 2000

Weiss, R.F., J.L. Bullister, R.H. Gammon, and M.J. Warner, Atmospheric chlorofluoromethanes in the deep equatorial Atlantic. Nature 314, 608-610, 1985

Appendix

Participants cruise SO-152

Monika Rhein	IUP Bremen	chief scientist
Dagmar Kieke	IUP Bremen	CTD analysis
Maren Walter	IUP Bremen	LADCP, vm-ADCP
Klaus Bulsiewicz	IUP Bremen	Chlorofluorocarbons CFCs
Gerd Fraas	IUP Bremen	CFCs, Helium, Tritium
Hilke Ötjen	IUP Bremen	CFCs, Helium, Tritium
Hemerson Tonin	Univ. Sao Paulo	CTD
Jorge Luiz Mesquita de Medeiros		Brazilian Navy
Walter Zenk	IFM Kiel	CTD
Hergen Johannsen	IFM Kiel	Nutrients, oxygen
Tom Avsic	IFM Kiel	CTD
Uwe Richter	IFM Kiel	Methyljodide
Karen Stange	IFM Kiel	Methyliodide
Anett Pfauder	IFM Kiel	Methyliodide
Robin Keir	GEOMAR Kiel	Methane
Karin Fürhaupter	GEOMAR Kiel	Methane
Carol Chin	OSU, USA	Methane, heavy metals
Toralf Heene	IOW Warnemünde	CTD, LADCP
Jutta Dankert	IOW Warnemünde	CTD
Mike Sommer	IOW Warnemünde	CTD, Salinometer
Stefan Schäfer	IOW Warnemünde	Helium, Tritium
Markus Potschantek	IOW Warnemünde	CTD
Thomas Badewien	IOW Warnemünde	CTD, Oxygen

IUP Bremen:
Institut für Umweltphysik der Universität Bremen
Abt. Ozeanographie
Kufsteiner Straße, Geb. NW1
28359 Bremen
Germany

GEOMAR Kiel
Wischhofstraße 1-3
24148 Kiel
Germany

IOW Warnemünde:
Institut für Ostseeforschung Warnemünde
Seestraße 15
18119 Rostock-Warnemünde

Univ.Sao Paulo:
Laboratorio de Modelagem dos Oceanos
Instituto Oceanografico
Universidade de Sao Paulo
Praca do Oceanografico
05508 Sao Paulo, SP
Brazil

OSU:
College of Oceanic and Atmospheric Sciences
Oregon State University
104 Ocean Admin. Building
Corvallis, OR 97331-5503
U.S.A.